

Final Report

DOE Award Number DE-FG02-02ER45964

Electromagnetic Properties of Matter at X-Ray Wavelengths

Principal Investigator:	David Y. Smith
Project Period:	1/1/02 - 12/31/06
Recipient Organization:	University of Vermont Burlington, VT 05405

Table of Contents

1. Summary	3
2. Background	4
3. Magneto-optics Dispersion Relations Between XFR and XMCD	5
4. Moments Representation of the Refractive Index of Transparent Materials	8
5. Optical – UV/Soft-X-Ray Characterization of Glass	9
6. UV/Soft-X-Ray Absorptions and Refraction in Silicate Glasses	11
7. IR Absorptions and Experimental Tests of Moments/Dispersion Analysis on $\text{TiO}_2\text{-SiO}_2$ Glass	14
8. Optical Pulse Propagation in Dielectrics	16
9. Optical and X-Ray Optical Properties of Silicon	18
10. Stopping Power of Light Elements for Charged-Particle Radiation	20
11. Literature Cited	24
Appendix A Publications	27
Appendix B Student and Postdoctoral Training	30

1. Summary of DOE Laboratory-Partnership Research Project

We have studied current issues involving photon and charged-particle interactions with matter in collaborations with researchers at Argonne and Brookhaven National Laboratories. Theoretical studies were carried out with Dr. Mitio Inokuti at Argonne and experimental work involved Dr. Christopher Homes at Brookhaven. A major goal was to extend the study of electromagnetic properties to as wide a spectral range as possible. Such a broad view of the E-M response discloses systematic trends not apparent in isolated measurements. Further, it allows one to exploit the power of dispersion analysis and sum-rule constraints. Emphasis was largely on UV and X-ray processes and in this we capitalized on the wide range of photon energies available at NSLS.

A key discovery was that, under favorable circumstances, dispersion theory allows one to relate dispersive processes, e.g. refractive index, to *spectral moments* of absorptive processes. This appears to be a new and insightful method in optics; it yields significant simplifications and provides a precise, model-independent way to characterize optical materials.

Problems addressed included a) x-ray magnetooptics; b) UV/soft-x-ray processes in insulators and their contribution to visible dispersion; c) demonstration of moments/dispersion analysis in glasses and applications to fiber-optic systems; d) the optical constants of silicon and their application to the stopping power of silicon for charged-particles. In summary:

- We resolved a long-standing conflict over the relation between x-ray Faraday rotation and x-ray magnetic circular dichroism. Specifically, accounting for the breaking of time-reversal symmetry by the magnetic field yields better fits to experiment. This seemingly esoteric issue is important for accurately deriving energy-level splittings from Faraday measurements, a common procedure in studies of magnetic materials for applications from motors to computers memories.
- We discovered that the optical properties of dielectrics in their region of transparency are determined by a series expansion in spectral moments of the dielectric's infrared and ultraviolet absorption spectra. We applied this to silicate glasses and clarified the role of "glass modifiers" in introducing charge-transfer, intra-ionic and perturbed-exciton transitions that combine to determine visible optical properties. Roughly, the refractive index is determined by the total electronic absorption, while dispersion depends on how the absorption is distributed.
- We applied the moments methods to pulse propagation in optical fibers and showed that signal distortion is minimized at the carrier-wave frequency for which dispersion in group velocity caused by IR processes just cancels the dispersion caused by UV and soft-x-ray processes.
- We applied the method of self-consistent dispersion analysis to construct a tentative composite set of optical constants for silicon using all optical and EELS measurements accessible in the literature. This has clarified outstanding issues regarding the scaling of relative measurements at the K edge and the accuracy of measurements at the L edge. Using this composite,
- We calculate the stopping power of silicon for charged particles as outlined by Bethe, a task not previously feasible for want of dielectric function data. This allowed us to resolve a conflict between measured values that was an issue for radiation damage and shielding applications.

2. Background

As originally conceived, this project involved a Laboratory Partnership with Dr. S. K. Sinha at Argonne National Laboratory collaborating on optical properties of matter, especially at X-ray wavelengths. However, between submission and the award, Dr. Sinha received, and accepted, an offer of a professorship in physics at the University of California San Diego. In consultation with Dr. Sinha, it was decided to continue the Partnership with Argonne, but in collaboration with an ANL colleague, Dr. Mitio Inokuti of the Physics Division who is an expert in the interaction of electromagnetic radiation with matter.

The field of the investigation remained essentially the same, but its scope was widened to include a combination of experimental and theoretical studies of the electromagnetic response of matter including optical and magnetooptical properties, stopping power of materials for ionizing radiation, and signal propagation in optical fibers. The theoretical parts of the study were carried out with Dr. Inokuti at Argonne, and the experimental portions with Dr. Christopher Homes at the National Synchrotron Light Source at Brookhaven National Laboratory.

The unique element of this work is the application of sum-rule and dispersion techniques to the analysis of optical and x-ray optical measurements. Historically these techniques originated in optical/atomic physics in the 1800s and early 1900s. However, their application to optics lagged and development passed to the high-energy physics community. A key goal of the project was to exploit these new developments in the analysis of optical measurements.

This approach to optical / x-ray-optical problems is timely because sum rules and dispersion relations are most valuable when data are available over a wide spectral range. Until recently this was not the case in optics, but development of synchrotron light sources has radically altered the situation; now accurate optical measurements can be made from the far IR to x-ray wavelengths on a single synchrotron source. This makes possible far more precise characterization of materials especially in terms of spectral moments of absorption, which have a closer connection to quantum models of matter.

Areas studied in this collaboration include

- Magnetooptic dispersion relations for x-ray Faraday rotation and x-ray circular dichroism
- Moments representation of the refractive index and a generalized Cauchy formula
- Applications of moments analysis to the optical and UV/soft-x-ray characterization of insulators
- UV/soft-x-ray absorptions and refraction in lead-silicate glasses
- IR absorption and experimental tests of moments/dispersion analysis in titanium-silicate glasses
- Optical pulse propagation in dielectric-fiber communications

- Silicon optical constants and the role of impurities and free-carrier absorption
- Stopping power of light elements for charged-particle radiation

A key discovery made early in the project was that under favorable circumstances dispersion theory allows one to relate dispersive properties such as refractive index – that arise from virtual quantum processes – to *spectral moments* of absorptive processes – that arise from real quantum processes. Since real processes are easier to treat conceptually, this leads to significant simplifications and provides a precise, model-independent characterization of material properties. Many of the projects treated after the first year relied heavily on this technique.

Reorganizing the research project with a new Argonne collaborator, setting up the collaboration with Brookhaven, and arranging synchrotron beam-line time delayed portions of the partnership research and required an extension of time. However, research momentum was maintained with the additional time devoted to enhancements such as application of our moments representation to fiber-optics communications, and to the determination of stopping powers. These were natural outgrowths of the original program and directly relevant to the interests of our DOE collaborators.

3. Magneto-optics dispersion relations between XFR and XMCD

A central issue in magnetic studies is the precise determination of magnetic energy level splittings. These are given directly by the MCD (magnetic circular dichroism) or difference in absorption for right- and left- circular light. However, in many instances it is experimentally easier to measure Faraday rotation, which is proportional to the difference in refractive index for right- and left-circular modes, and then to calculate the circular dichroism using dispersion theory. Until recently it was believed [Alp 1991, McWhan 1992 and 1994] that the difference of Kramers and Kronig's original dispersion relations provides the connection

$$\kappa_r - \kappa_l = -\frac{2}{\pi} E \mathcal{P} \int_0^{\infty} \frac{n_r(E') - n_l(E')}{E'^2 - E^2} dE' . \quad (1)$$

However, in connection with semiconductor studies it has been pointed out by Lidiard and coworkers [Boswarva1962, Bennett 1965] that in a magnetic field the dielectric response is a tensor – the Lorentz force creates off-diagonal response – and the circularly polarized normal modes of propagation result from diagonalizing this tensor. Although the Kramers-Kronig relations holds for each tensor element individually, diagonalization mixes diagonal and off-diagonal elements, but with phase differences of $\pm \pi/2$. Kramers-Kronig-like dispersion relations may then be recovered from symmetric and antisymmetric combinations of the optical constants [Smith 1976a] . Thus, one finds two sets of dispersion relations for the MCD,

Symmetric (sum) Relations:

$$\frac{\kappa_r(E) + \kappa_l(E)}{2} = -\frac{2}{\pi} E \mathcal{P} \int_0^\infty \frac{1}{E'^2 - E^2} \left[\frac{n_r(E') + n_l(E')}{2} - 1 \right] dE', \quad (2)$$

Antisymmetric (difference) Relations

$$\kappa_r(E) - \kappa_l(E) = -\frac{2}{\pi} \mathcal{P} \int_0^\infty \frac{E'}{E'^2 - E^2} [n_r(E') - n_l(E')] dE'. \quad (3)$$

The symmetric or sum form has the same structure as originally found for linear modes by Kramers and Kronig, so that, *on average*, the circular modes behave in the usual manner, i.e., their average is an odd function of energy. In contrast, the difference relation predicts that the magnetic circular dichroism should be an even function of energy; it satisfies a dispersion relation with a different structure. The fundamental point is that the magnetic field breaks time-reversal symmetry and use of symmetric and antisymmetric combinations sorts out the resulting complexity.

This situation was thrown into confusion by two measurements from highly regarded x-ray groups reporting experimental demonstrating that Eq. 1 is correct [Siddons 1990, Collins 1999]. Examples of the measured XMCD (x-ray magnetic circular dichroism) and XFR (x-ray Faraday rotation) at the L_3 edge of Fe_3Pt are given in Fig. 1. Qualitatively, the two measurements appear to satisfy Eq. 1, and calculated values of the XMCD from the XFR *via* Eq. 1 fit the measured values reasonably well. As similar calculation using the antisymmetrized form, Eq. 3, also gives a reasonable fit, indicating that, at the magnetic fields used, the splittings are not large enough for a simple comparison of line shapes to serve as a critical test of the alternative forms.

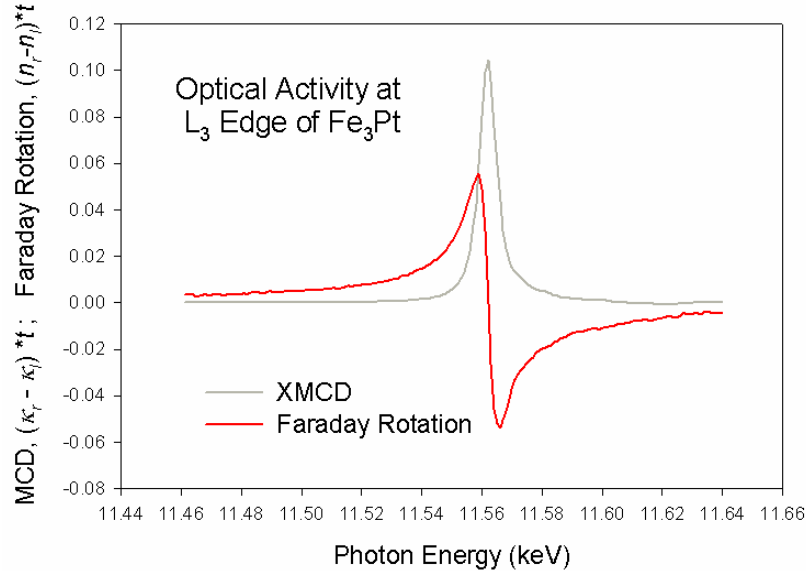


Fig. 1 X-ray magnetic circular dichroism and x-ray Faraday rotation at the L_3 edge of Fe_3Pt (courtesy of Dr.S. P. Collins, Daresbury Laboratory).

We have devised a more sensitive test by making use of the additional experimental observation

that the MCD goes to zero in the limit of zero frequency – at zero frequency the Lorentz force, and consequently all dynamic magnetic effects, go to zero . Taking this limit of Eqs. 1 and 3 by expanding their denominators in a Taylor series yields

$$\int_0^{\infty} [n_r(E') - n_l(E')] dE' = 0 ,$$

if Eq. 1 holds. In contrast,

$$\int_0^{\infty} \frac{n_r(E') - n_l(E')}{E'} dE' = 0 ,$$

if Eq. 3 holds.

These two integrals may be evaluated directly from the XFR measured by Collins with the result

$$\frac{\int_0^{\infty} \frac{n_r(E') - n_l(E')}{E'} dE'}{\int_0^{\infty} \left| \frac{n_r(E') - n_l(E')}{E'} \right| dE'} = 1.5 \times 10^{-4} \quad \text{vs.} \quad \frac{\int_0^{\infty} [n_r(E') - n_l(E')] dE'}{\int_0^{\infty} |n_r(E') - n_l(E')| dE'} = -2.0 \times 10^{-3}.$$

Here we have normalized the integrals to their absolute areas to place them on an equal footing.

Both integrals are show a large degree of cancellation between positive and negative parts of the XFR, but the integral corresponding to the antisymmetrized dispersion relation, Eq. 3, is more than an order of magnitude smaller than that for Eq. 1, in strong support of Eq. 3. Thus, we conclude that this further analysis verifies the applicability of the symmetrized dispersion relations, Eqs. 2 and 3, for circular modes in the presence of a magnetic field. The comparisons originally reported in the literature were simply not sensitive enough to detect the difference between the correct and incorrect forms

The writer wishes to thank Dr. Collins of the CLRC Daresbury Laboratory (Warrington, UK) for kindly providing his measured magneto-optic data so that this reanalysis could be carried out.

For further details, see [Smith 2003].

An important feature of this reanalysis was the use of the high- and low-energy limits of the dispersion relations to establish sum rules to test optical data. A byproduct of this was the realization that, under favorable circumstances, the resonant denominator in the Kramers-Kronig relations, $(\omega'^2 - \omega^2)^{-1}$ can be expanded in a Taylor or Laurent power series to yield a highly convergent power-series representation of parameters describing linear response. This technique should be useful in many fields involving linear response. As an example, we considered a classical problem in optics, the representation of the refractive index of transparent materials as described in the next section. The results give a fundamentally new way of understanding optical properties using a moments representation. The approach is reminiscent of Van Vleck's moments analysis of spin-resonance experiments [Van Vleck, 1948], but it does not appear to have been previously applied to optics problems.

4. Moments Representation of Refractive Index of Transparent Materials

The absorption spectra of a typical transparent substance, vitreous silica, is shown in Fig. 2. Provided the silica is pure, absorption is negligible from 0.35 eV in the IR to 7.6 eV in the UV. The Kramers-Kronig equation for the real part of the index, $n(\omega)$, in terms of the extinction coefficient, $\kappa(\omega)$, is

$$n(\omega) - 1 = \frac{2}{\pi} P \int_0^{\infty} \frac{\omega'}{\omega'^2 - \omega^2} \kappa(\omega') d\omega' \quad (6)$$

But, in the region of transparency between the highest IR frequency, ω_{IR} , and the lowest UV frequency, ω_{UV} , $\kappa = 0$, so the integral may be divided into two parts, one covering the IR (in red) and the other covering the UV (in blue):

$$n(\omega) - 1 = \frac{2}{\pi} \int_0^{\omega_{IR}} \text{IR absorption } d\omega' + \frac{2}{\pi} \int_{\omega_{UV}}^{\infty} \text{UV absorption } d\omega' , \quad \omega_{IR} < \omega < \omega_{UV}. \quad (7)$$

Provided we restrict our interest to a representation of $n(\omega)$ to the region of transparency, the integrands are never singular and the denominators may be expand in power series, the UV integral in a Taylor series and the IR integral in a Laurent series. The result is an *exact* power-series expansion

$$n_{\text{transparent}}(\omega) = \dots + \underbrace{n_{-4}\omega^{-4} + n_{-2}\omega^{-2}}_{\text{ionic terms}} + \underbrace{n_0 + n_2\omega^2 + n_4\omega^4}_{\text{electronic terms}} + \dots, \quad \omega \text{ in transparent region}. \quad (8)$$

The coefficients are moments of the IR and UV absorptions that are directly related to ionic vibrational modes and electronic band structure; they are *not* fitting parameters. Examples are:

$$n_{-2} = -\frac{2}{\pi} \int_{IR} \omega' \kappa(\omega') d\omega' , \quad \sim \text{IR oscillator strength} \quad (9)$$

$$n_0 = 1 + \frac{2}{\pi} \int_{UV} \frac{1}{\omega'} \kappa(\omega') d\omega' , \quad \text{Inverse 1}^{\text{st}} \text{ moment of UV absorption} \quad (10)$$

$$n_2 = \frac{2}{\pi} \int_{UV} \frac{1}{\omega'^3} \kappa(\omega') d\omega' . \quad \text{Inverse 3}^{\text{rd}} \text{ moment of UV absorption.} \quad (11)$$

The important point is that Eq. 8 is very general assuming only a causal, linear optical response described by analytic functions. It is independent of detailed models of the material and should

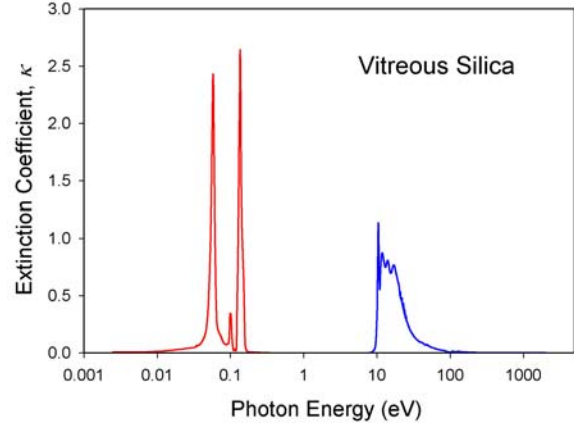


Fig. 2 The absorption spectrum of vitreous silica. Absorption is negligible from the IR to the UV.

not be confused with parameterized fittings; the expansion coefficients are well-defined function of the spectrum of real quantum processes and allow for any spectral distribution of absorption. This distinguishes the present result from treatments such as the classical Sellmeier model for optical constants that relies on a small number of electromechanical oscillators. Tests of a variety of published glass data show that Eq. 8 provides a simpler and more accurate representation of the index than the widely used Sellmeier model [Black 2005]. Moreover, within the region of transparency, the expansion is highly convergent. An example of this for vitreous silica is given in Fig. 3.

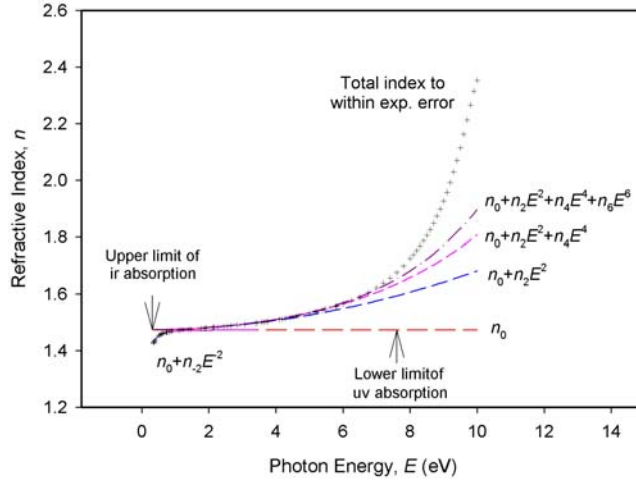


Fig. 3. Absorption moment contributions to the refractive index of vitreous silica as calculated from the absorption data of Philipp [Philipp 1985].

Historically, a partial expansion starting with $n_0 + \dots$ was first suggested by Cauchy [Cauchy 1836] on the basis of the ether theory of light. But, Cauchy's treatment was found to be wanting both because it lacked the negative exponent terms that account for ionic polarization (an source of dispersion unknown at the time) and because it did not predict anomalous dispersion. Moreover, with the demise of the ether theory of light, Cauchy's treatment was dismissed as completely misguided.

However, the present work shows that, with the addition of ionic-polarization terms, a generalized Cauchy representation of the refractive index is exact *within the region of transparency* of a dielectric. Moreover, the series is highly convergent in many important applications. In brief, Cauchy got the mathematics right because his physical model of light was linear and causal, even though the model was wrong in detail.

For further details, see [Smith 2002, Smith 2004].

5. Optical - UV/Soft X-ray Characterization of Glass

An attractive test-bed for the new moments representation of the index is the large empirical data base available for optical glass. Traditionally, the properties of optical glass are defined by

technologically useful combinations of the refractive index at several wavelengths spanning the visible [Schott 1965] . These include the index, n_d , at the Fraunhofer d line, the mean dispersion, $n_F - n_C$, or difference in index between the F and C lines, and the Abbé number, an alternative measure of dispersion relative to $n_d - 1$. The results of applying moments analysis to our exemplary substance, silica, are summarized here.

- The measured index at the Fraunhofer d line is in excellent agreement with that calculated from absorption moments when two IR terms and three UV/soft x-ray terms are included in the generalized Cauchy expansion. The inverse-first moment, n_2 , of the electronic absorptions in the UV/soft-x-ray region account for 99% of the index itself. In contrast, IR contributions are less than 0.1% of the index. This explains the common, but erroneous (see below), notion that the optical properties of insulators are determined essentially only by electronic processes.
- The mean dispersion is independent of the inverse-first moment, n_2 , of the electronic absorptions and, hence, is largely independent of the index n_d . Electronic processes are still large with the inverse-third-moment term, n_4 , contributing 86% of the mean dispersion. However, infrared processes play a remarkably larger role than in the index, with the first moment of the IR ionic vibrational spectrum contributing 9% of the dispersion. A second point is that this IR contribution is positive, and hence, increases the dispersion; in contrast, the ionic vibrations make a negative contribution to the index. As we show below, the IR dispersion is crucial for long-distance fiber-optic communication. Without it, signal distortion would be overwhelming.

Taken together, the above two points explain why empirical models of glass chemistry based on ionic polarizability are reasonably accurate for predicting the index, but fail to predict dispersion accurately. These models simply do not adequately account for the spectral distribution of oscillator strength.

- The Abbé number, a relative measure of dispersion, is determined primarily by the ratio of inverse-first to inverse-third moments of the UV/soft-x-ray spectrum, which account for 83% of its value. That is, relative to the index, the dispersion depends primarily on the *distribution* of electronic oscillator strength over the UV and soft-x-ray spectrum, not on its magnitude. As with the dispersion itself, the IR vibrational spectrum is responsible for roughly a tenth of the Abbé number.

In engineering practice, glasses of different dispersion have been developed by “cut-and-try” addition of various metal oxides or “glass modifiers” to the “glass former,” commonly silica. From the vantage point of our moments representation, these metal ions alter the *distribution* of oscillator strength in the electronic absorption spectrum at UV and soft-x-ray wavelengths both by introducing inner-shell transitions and by rearranging the valence-shell bonds with oxygen atoms. [Specific examples from the current work are given in Sections 6 and 7].

As far as the writer knows, the glass research community continues to rely on traditional glass models dating from the 19th and early 20th century that are based on the classical notion of fixed polarizable ions. Advances in synchrotron-source spectroscopy have rarely been exploited. The principal exception are the UV studies of Izumitani (Hoya Glass Co., Japan) [Isumitani 1986] that used both arc and synchrotron sources (such as Spring 8) to measure the reflectivity of glass.

Unfortunately, Izumitani did not have the analytic framework developed here to analyzing his measurements, so his conclusions remained qualitative. We have, however, analyzed several sets of Izumitani's data for which there are measurements over a sufficiently wide energy range and have obtained quantitative insights [See Section 6].

For further details, see [Smith, 2002].

6. Ultraviolet/Soft-X-Ray Absorptions and Refraction in Silicate Glasses

As an example of the utility of our moments / dispersion analysis, the UV reflectivity spectra of Izumitani for selected silicate glasses were analyzed for their absorption spectra and these, in turn, used to calculate the UV/soft-x-ray contribution to refraction at visible wavelengths.

The resulting absorption spectra for crystalline and vitreous silica, as well as for soda and lead glass are shown in Figs. 4 and 5. These illustrate the electronic perturbations that both structural disorder and modifier ions have on the absorption of the glass former. The primary effects are:

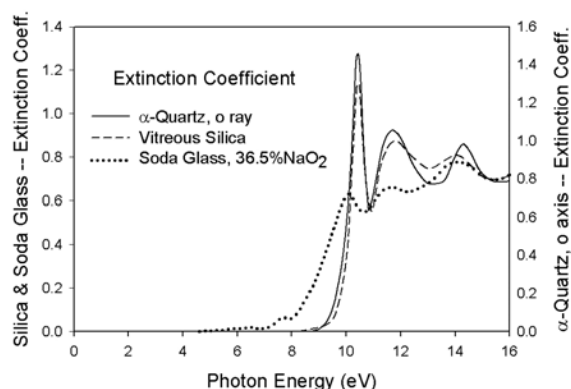


Fig. 4 Comparison of extinction coefficients for α -quartz (o ray), vitreous silica and soda glass.

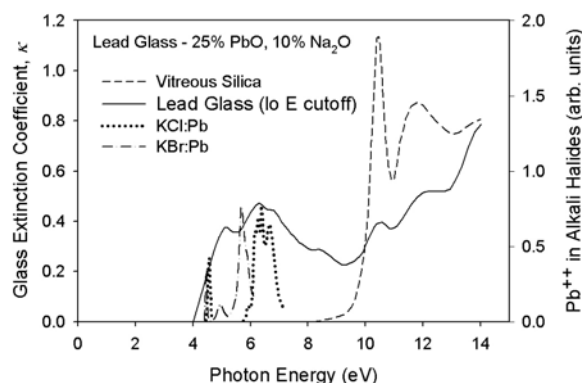


Fig. 5 Extinction coefficient for vitreous silica, lead-soda glass and absorption of Pb^{++} ions in alkali halides.

- **Structural disorder** – Both crystalline and glassy silica consist of corner-sharing SiO_4 tetrahedral units. In crystalline forms the tetrahedra link to form ordered lattices with the corner oxygen atoms bridging the central silicon atoms. In vitreous forms, the tetrahedra join to form a random network. Fig. 4 shows that the optical absorption [Philipp 1985] of α -quartz and vitreous silica are remarkably similar. The more energetic transitions are somewhat broadened in the vitreous state, the 11.7 eV transition (an interband excitation) and the 10.4 eV absorption (the corresponding exciton) are nearly independent of long-range spatial order. This is consistent with excitations of bridging-oxygen bonds within SiO_4 tetrahedra for which the bond energy is largely independent of how the tetrahedral are arranged.

- Compositional Disorder / Perturbed Excitons & Charge-Transfer Transitions – In contrast to structural disorder, the absorption of silicate glass containing Na₂O shows that compositional disorder caused by addition of the Na₂O modifier has profound effects:

1. Absorptions of SiO₄ tetrahedra are broadened, shifted, and weakened (the latter by dilution).
2. A strong absorption develops on the low-energy side of the 10.4 eV exciton, and
3. A weak absorption band appears at 7.5 eV.

Lithium glass exhibits a similar spectrum [Izumitani 1986].

Since the oxygen-silicon ratio in alkali-containing glasses is greater than two, part of the oxygen atoms that are bound to silicon atoms as non-bridging oxygens (NBOs) with bonds terminated by sodium atoms. The bond energies and absorptions of the SiO₄ tetrahedra with NBOs will be perturbed depending on how the NBOs are terminated. In particular, sodium ions will perturb the absorptions of neighboring SiO₄ units containing non-bridging oxygens. As a first approximation this can be viewed as a perturbed exciton at sites where sodium replaces silicon, or almost equivalently, as an excitation involving Na-O bonds. {To test this, we calculated absorption energies of the hypothetical structure ≡Si–O–Na (as H₃Si–O–Na) using the Gaussian code [Frisch 1995]. For the Na-O bond lengths of 1.9 to 2.5 Å predicted by MD simulations, excitation energies range from 7.6 to 8.9 eV, in reasonable agreement with the broad absorption seen on the exciton's low-energy flank.}

The sodium-associated 7.5 eV band is weak and only resolved in reflectivity for samples with 29% or more Na₂O. It gains strength rapidly with concentration and is well resolved at 36.5% Na₂O. Speculation that the absorption involves Na-O bonds or charge transfer to an Na⁺ ion seems inconsistent with its low oscillator strength. The apparently super-linear concentration dependence suggests that complexes of Na⁺ ions or NBOs are involved. Hirota *et al.* [Hirota 1985] attributed the band “to the non-bridging oxygen ions produced by the presence of Na⁺ ions.” Alternatively, several absorptions seen in irradiated silica lie near 7.5 eV [Pacchioni 2000]. In oxygen-deficient silica, a 7.6 eV absorption is attributed to Si-Si bonds at neutral oxygen vacancies [Griscom 1985]. In oxygen-surplus silica, the peroxy bridge (≡Si-O-O-Si≡) and the peroxy radical (a hole trapped at a peroxy bridge) have been associated with absorptions from 6.5 to 7.8 eV [Pacchioni 1998]. The Si-Si bond seems unlikely in alkali glasses, which contain enough oxygen to fully bond all silicons. However, the presence of several NBOs coordinating an alkali ion suggests that peroxy bridges may form between adjacent NBOs. Thus, the 7.5 eV band likely involves excitation of interacting NBOs neighboring an alkali ion.

- Compositional Disorder and Intra-ionic Absorptions – Fig. 5 gives the absorption of lead-sodium-silicate glass. As in soda glass, the silica absorptions are broadened and weakened. In contrast, prominent absorptions appear from 4 to 7 eV. For comparison we give the A, B and C bands of Pb⁺⁺ ions in KCl and KBr at LN temperature [Fukuda 1964]. Aside from broadening, the lead-glass and lead-doped-alkali-halide spectra are virtually identical in this range. In alkali-halide hosts, Seitz [Seitz 1938] identified these absorptions as intra-ionic 6s²→6s6p transitions of the divalent ion. This also appears to apply here. The broadening reflects either Pb⁺⁺ sites with random short-range order, or several alternative sites with well-defined, but different local coordinations. (This explanation is inapplicable to the weak 7.5 eV band in soda glass; the lowest excitation energy of Na⁺ ions is roughly 30 eV [Moore 1971].) The second new feature in Fig. 5 is a small band at approximately 8.4 eV superimposed on the broadened SiO₄ exciton. A similar absorption, the D band, is seen for Pb and Tl ions in alkali-halide hosts, and has been

attributed to a perturbed exciton [Fukuda1964, Yuster 1953]. Excitation of a Pb-O bond is an alternative description, but that may be viewed as a severely perturbed exciton at a site where Pb replaces Si.

In summary, this analysis of the UV/soft-x-ray spectra of glasses shows that the glass modifiers employed in optical glass produce absorptions in the ultraviolet that are analogous to classic color centers seen at visible wavelengths in ionic solids containing defects formed by chemical or radiological treatment. Absorptions include intra-ionic and charge-transfer transitions, and perturbed of host excitons. These absorptions largely determine the index in the visible, which is predicted to within a few percent from the UV spectrum by our generalized Cauchy dispersion formula.

It is the writer's belief that the study of the UV and soft-x-ray spectra of glasses, which is now possible with synchrotron sources, holds considerable promise. Knowledge of the electronic absorption of a select number of binary and ternary glasses as function of composition should provide the basis for understanding the bewildering complexity of the visible optical properties of multi-component glasses as a function of composition. Presently these are explained with *ad-hoc* classical or empirical models that have modest predictive value, and development of glass with specific properties still depends on compounding and testing large number of trial compositions. The present development of a moments representation for the index appears to provide the basis for a system of rational materials engineering of the optical properties of glass.

A second observation is that measurements of optical properties at UV and soft-x-ray wavelengths should be possible by reflectivity even from the surface of liquid samples. While the black-body radiation of silicate melts is overwhelming in the IR and visible, it is negligible in for UV and shorter wavelengths. This opens the possibility of *in situ* determination of the composition of glass melts as they are being produced, a procedure that could be of practical value in quality control in the glass industry.

While the present study concerns optical glasses, for which large data bases are available, many of the observations concerning the modifier-ion specific UV spectra apply to radioactive-waste glasses. Knowledge of the UV spectra of the waste ions could potentially be useful for non-destructive determination of waste composition and monitoring. The practical drawback to this application is that the spectra arising from the large range of elements present in waste may well overlap to such an extent that it would be difficult to detect specific elements in low concentration. Considering its very rich absorption spectrum, iron from the stainless-steel fuel rod cladding is of particular concern.

For further details, see [Smith 2004].

7. Infrared Absorptions and Experimental Tests of Moments/Dispersion Analysis on TiO_2 – SiO_2 Glass

To demonstrate the value of absorption measurements over a broad spectral range proposed in the preceding section, reflectivity measurements were carried out on a simple binary glass consisting of vitreous SiO_2 containing 7.4 wt percent of TiO_2 . This glass was chosen in consultation with Prof. S. Jacobs of the Institute of Optics at the University of Rochester, who kindly provided us with samples. The glass is remarkable for its vanishingly small coefficient of thermal expansion, and is prepared commercially by Corning as ULETM (Ultra-Low Expansion) glass by pyrolysis of high-purity gaseous precursors. This was important for our purposes since the resulting material is remarkably free of impurities with the exception of trace amounts of OH^- ions introduced by the pyrolysis.

Experimental measurements were carried out at the National Synchrotron Light source at Brookhaven National Laboratory in collaboration with Dr. Christopher C. Homes of Brookhaven's Physics Division. Reflectance measurements were made over a continuous range from the far IR to the UV (18.3 to $32,000\text{ cm}^{-1}$), a factor of almost 2000 in energy that appears to be a record for glass studies. These measurements were augmented with literature values of the VUV reflectivity from 2.3 to 12.2 eV reported by Izumitani [Izumitani 1985], and Osantowski's values [Osantowski 1974, Rife 1980] from 11.8 to 41.3 eV. Philipp's silica data [Philipp 1985] were used as a high-energy extrapolation. The optical constants were calculated by Kramers-Kronig analysis, with direct measurements of the refractive index at the Fraunhofer C, D, and F lines [Corning 2004] used to anchor the refractive index.

The results in the regions of IR and UV absorption are shown in Figures 6 and 7; the intervening region is absorption free.

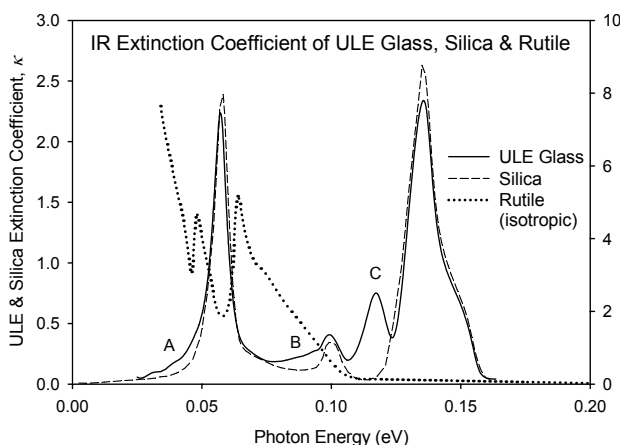


Fig. 6 IR absorption of SiO_2 with 7.4 wt% TiO_2 . Absorptions caused by titanium marked as A, B and C.

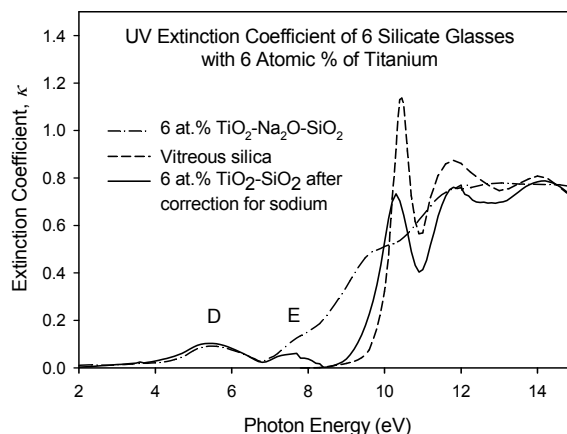


Fig. 7 UV absorption of SiO_2 with 7.4 wt% TiO_2 . Titanium-associated bands are marked D and E.

• **Infrared Absorption** The IR extinction coefficient of ULE glass for our composite reflectivity is shown in Fig. 6 together with those for vitreous silica [Philipp 1985] and rutile [Ribarski 1985], the usual crystalline form of TiO_2 with octahedrally coordinated titanium. The observed spectrum is remarkably similar to that for vitreous silica, and shows no indication of

rutile inclusions. The principal titanium-associated IR absorption is the prominent band at $\sim 950 \text{ cm}^{-1}$ lying just below the host silica's strong 1076 cm^{-1} band. Other titanium-associated absorptions occur in broad bands at $240 - 400 \text{ cm}^{-1}$ and $650 - 730 \text{ cm}^{-1}$. These lie just below the host-silica absorptions at 450 and 800 cm^{-1} . This close association with the titanium induced absorptions and the host silica spectra strongly suggests that the titanium ions simply perturb the silica absorptions. Further, the lack of any trace of rutile-like absorptions, which would imply octahedral coordination, suggests that the titanium is tetrahedrally coordinated in the glass. (Titanium ions are known to assume either octahedral or tetrahedral coordination in minerals.) In short, titanium substitutes for silicon as Ti^{4+} ions in the random network of the glass.

Substitution of Ti^{4+} for Si^{4+} creates four Ti–O–Si bonds, i.e., an isolated TiO_4 tetrahedron with oxygen bridges to four neighbouring SiO_4 tetrahedra. The frequency of modes involving Ti–O–Si bonds (or tetrahedra with these bonds), will be lower because of the greater mass ($m_{\text{Ti}}/m_{\text{Si}} = 1.17$) and the strength reduction by 0.862 of the Ti–O bond [Nakamoto 1997]. In particular, the prominent IR-active bands of pure silica are ascribed to TO modes of the SiO_4 network having substantial motion of the light oxygen ions. From the known geometry of these modes [Bell 1974, Kirk 1988], we can assign the prominent C peak to the asymmetric stretching mode of the Ti–O–Si bond; the weak B band to a combination of Ti–O–Si in-plane bending and symmetric stretching modes; and the A band to the Ti–O–Si out-of-plane rocking modes.

An important observation relative to the moments formalism is that the area (roughly the oscillator strength) of the IR spectrum is not significantly changed. The silica peaks become weaker, but the area they lose reappears in the titanium peaks. To first order, this means that the IR contribution to the index in the visible is not changed by the admixture of TiO_2 . As will be seen below, this is in sharp contrast to the effect of titanium on the UV/soft-x-ray spectrum.

- The UV extinction coefficient for our titanium glass is compared with that of vitreous silica [Philipp 1985] in Fig. 7. These results are approximate since our measurements and literature data were pieced together to form a composite. The most prominent UV features are the strong charge-transfer absorptions lying below the silica exciton peak at $\sim 10.4 \text{ eV}$ [Philipp 1985]. Absorption rises sharply after $\sim 4.5 \text{ eV}$ and reaches a maximum between 5.5 and 6 eV . A secondary maximum lies between 7.4 and 7.8 eV on the low-energy flank of the broadened host-silica exciton. We interpret these two absorptions as charge-transfer transitions primarily localized at TiO_4 tetrahedra. Qualitatively, an electron is transferred to the central titanium ion to create a Ti^{3+} leaving a hole shared by the tetrahedral cage of O^{2-} ions, i.e., a localized exciton.

Compared with the IR absorption, the titanium addition creates a very large redistribution of absorption strength toward lower energies. The silica exciton at $\sim 10 \text{ eV}$ is weakened significantly and strong new transitions appear at ~ 5 and $\sim 7 \text{ eV}$. While this leads to only a few percent change in the index, n_d , the dispersion, δ_{FC} , increases by 28%. This illustrates the crucial dependence of the dispersion on the distribution of the electronic absorptions in insulators. This important aspect of dispersion is not evident in traditional optical-property models.

For further details, see [Smith 2007 (in press)].

8. Optical Pulse Propagation in Dielectrics

The moments formulation of the index provides clear insights into pulse propagation in dielectrics, especially in communications applications. Pulse distortion in optical fibers has two source [Gloge 1971]: 1. differences in propagation times of the EM modes supported by the fiber, and 2. distortion of pulse shape because of refractive-index dispersion for the pulse's various frequency components. The first can be eliminated by using single-mode fibers; the second can only be minimized by the choice of fiber dielectric. Traditional descriptions of the dielectric's material dispersion are based on discrete mechanical-oscillator optical models and empirical chemical descriptions of the glass [DiDomenico 1972, Wemple 1979]. While sufficient for qualitative work, they do not provide fundamental insight and are cumbersome.

However, starting from a generalized Cauchy description of the optical-fiber dielectric, the group velocity and its derivatives – which parameterize pulse distortion – can be simply described in terms of moments of dielectric's IR and UV/soft-X-ray absorption spectra. In turn, these moments are directly related to the specific absorptions of the chemical components glass former and modifiers of the fiber optic-core. This is most easily visualized by introducing the concept of *group refractive index*, n_g , which we define so that the group velocity is given by c/n_g , where c is the velocity of light. The minimum pulse distortion occurs for the carrier frequency at which n_g is a minimum. An example for vitreous silica is shown in Fig. 8.

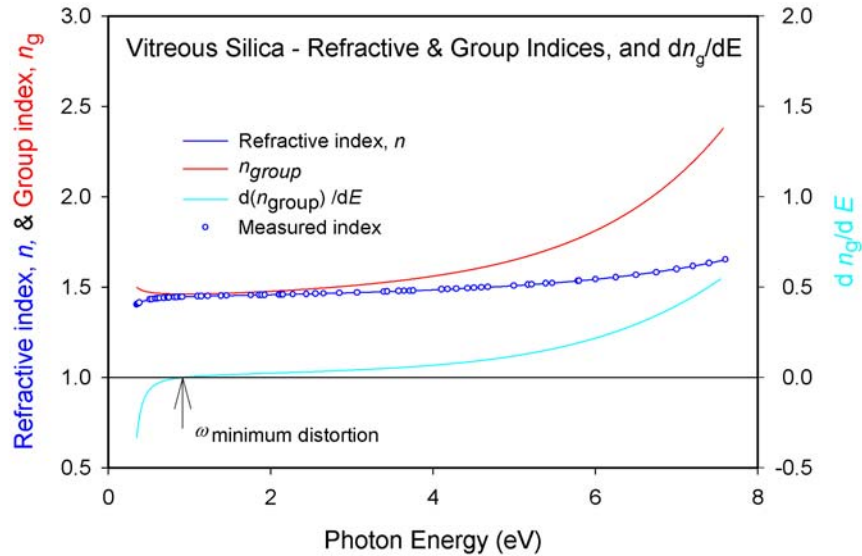


Fig. 8 The measured refractive index of vitreous silica fit with the Generalized Cauchy formula, and the corresponding group index, and its derivative showing the frequency for minimum pulse distortion.

Differentiation of the moments expression for the group velocity yields a simple formula for the carrier-wave frequency for minimum pulse distortion.

$$\omega_{\min} = \sqrt[4]{\frac{n_{-2}}{3n_2}} \quad (12)$$

This can be interpreted as showing that the carrier-wave frequency for minimum distortion depends on the **balance** of **two** quantities, n_2 , the first moment of the IR absorption (shown in red) and n_2 , the inverse third moment of the UV/soft-x-ray absorption (shown in blue). Specifically, the negative dispersion in the group velocity arising from polarization by IR modes just balances the positive dispersion arising from polarization by UV modes.

It also brings out the point that pulse distortion can only be minimized because of both IR and UV modes contribute to dispersion in the group index, but with opposite sign. In a nonpolar material, there would be no IR absorption and it would not be possible to find a minimum carrier frequency. In short, long-distance fiber optics communication only works because glasses have ionic vibrational modes.

In practice, Eq. 12 can be approximated by a simple expression

$$\omega_{\min} \sim \text{Average Electronic Excitation Energy}^4 \sqrt{\frac{\text{Vibrational Absorption-Band Area (Oscillator Strength)}}{\text{Electronic Absorption-Band Area (Oscillator Strength)}}}, \quad (13)$$

where we have introduced

$$[\text{Average Excitation Energy}]^4 = \int_{\text{UV}} \frac{1}{\omega'^4} \omega' \kappa(\omega') d\omega' \bigg/ \int_{\text{UV}} \omega' \kappa(\omega') d\omega'. \quad (14)$$

The point of Eq. 13 may be seen from comparing the doped and undoped absorption spectra for titanium-silicate glass experiment, Figs. 6 and 7. For both IR and UV absorptions, doping produced redistribution of band area, but very little total area change; the quantity beneath the radical sign is only weakly dependent on doping. Thus, for a given glass former, the dominant factor determining the optimum frequency is the average electronic excitation energy.

For example, in vitreous SiO_2 , the electronic excitation energy can be changed by adding glass modifiers, such as TiO_2 or PbO_2 ; these modifiers introduce ionic absorptions (e.g., from Ti^{4+} as in Fig. 7) in the host's band gap and lower the average electronic energy. The modifiers tend to redistribute, but not greatly alter, the vibrational and electronic absorption-band areas, so they have negligible effect on the second (ratio) term in the equation, which is primarily dependent on the glass former.

The physics of minimum distortion may be further clarified by considering the pulse group velocity. Both the vibrational and the electronic polarization contribute to the pulse delay. Only at the minimum of pulse distortion are the contributions equal. This can be understood by observing that within the dielectric an EM pulse actually consists of a compound polariton, a linear combination of electromagnetic, ionic-polarization, and electronic-polarization waves. Minimum distortion of the pulse obtains when the ionic polariton and the electronic polariton, considered separately, have the same group velocity. That is, the pulse moves at the same velocity in each subsystem.

For further details, see [Smith 2007 (in press)].

9. Optical and X-ray-Optical Properties of Silicon

Silicon's unique optical and x-ray-optical properties lie behind a host of its technological applications – photodetectors and photovoltaic cells in the case of the IR and visible properties, particle detectors that utilize Coulomb excitation of core shells, and charged-particle energy loss in radiation shielding made of silicate materials that depend on x-ray absorption.

This said, there are major gaps in the measurements of these properties: Although K-shell absorption is known to high precision above ~ 2600 eV, there are no absolute measurements at the K edge, only relative spectra. Although there are many reports of L-edge spectra, there appear to be *no* measurements from 277 to 1486 eV, the bulk of the L-shell range; and virtually all the IR refractive index data in the literature were obtained on impure samples and, as detailed below, in the far IR free-carrier effects swamp the intrinsic properties leading to misleading optical data.

In light of these problems and because of conflicting values of the stopping power of silicon for charged particles, Dr. Inokuti, a long term member of the ICRU (International Commission on Radiation Units and Measurements) encouraged developments of a composite optical data set for silicon using dispersion techniques and sum-rule / moments constraints. We therefore reviewed the silicon literature with emphasis on direct optical experimental measurements and developed a database of measurements from the far IR to the x-ray region. It consisted of transmission measurements on films and thinned samples for UV and soft x-ray photons, reflectivity in the visible and far UV, transmission and refractive index measurements in the IR.

Since none of these properties can be measured over the full spectral range in condensed matter, analysis requires a self-consistent extension of the Kramers-Kronig analysis. In this procedure a convenient quantity, such as reflectance, is estimated from the available measurements over the whole energy range. A K-K analysis is then performed to obtain tentative values of all optical constants. These tentative values are corrected using the measured values. The starting quantity is then recalculated and the procedure iterated until it converges to fit all the measurements. The results are then tested using known quantum-mechanical sum rules and for consistency with moments formulas discussed above to exclude experimental data with systematic errors. Our tentative results, composite Y, are shown in Fig. 9.

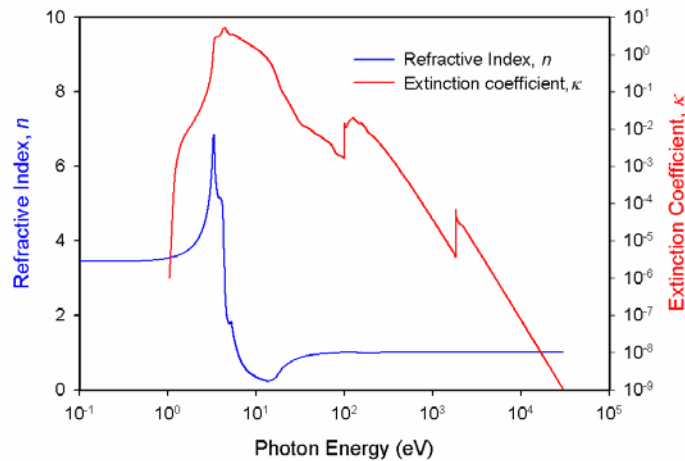


Fig. 9 Composite optical constants for crystalline silicon developed in this collaboration.

In developing this composite, an early finding was that virtually all of the reported silicon optical properties in the far IR properties refer to contaminated samples. The key to this discovery was our generalization of Cauchy's index representation: Intrinsic silicon is non polar and at low temperatures should exhibit virtually no absorption below the band-gap energy. Without IR absorptions there are no terms in *inverse powers* of E in the series for the index, so, in the limit of low energies, the refractive index within the band gap should be a linear function of photon energy squared. This is clearly the case in the near IR as shown in Fig. 10.

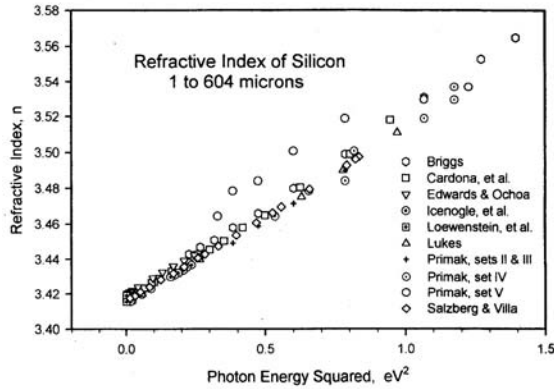


Fig. 10 Measurements of the refractive index of crystalline silicon for photon energies above 3 meV.

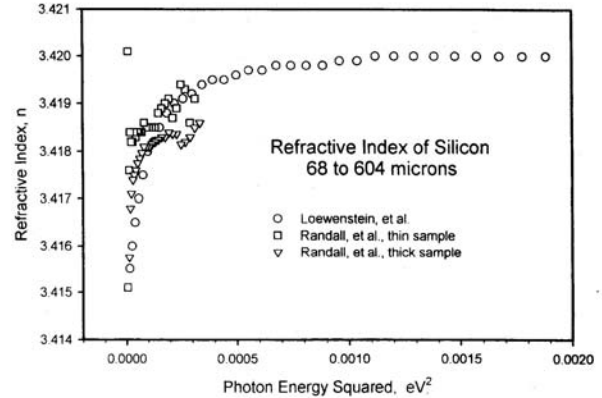


Fig. 11 Data from Fig. 10 plotted on an expanded scale below 20 meV to emphasize free carrier contamination.

However, at lower energies there is a dramatic drop in the index that can be traced to free-carriers arising from trace impurities as shown in Fig. 11. This is even found for modern microwave measurements that are claimed to be made on high-purity samples.

Fortunately, the moments formulation provides a simple way of sorting this out, and extracting both intrinsic properties and the free-carrier concentration: A fit of Eq. 8 gives both the free-carrier oscillator strength, via the coefficient n_{-2} , and the intrinsic index via n_0 and n_2 , etc. This procedure allowed us to analyze widely quoted measurements made at IBM by Schumann, *et al.* [Schumann 1970 and Schumann 1971] for which there was no simple analysis scheme available when the measurements were made. This work formed the basis of a senior thesis of a student in collaboration with Dr. William Karstens at St. Michael's College (Colchester, VT). The innovation of plotting the free-carrier-dominated energy region as an inverse function of photon energy squared is illustrated in Figs. 12 and 13 (next page) for the measurements of Schumann [Schumann 1970] and of Auslander and Hava [Auslander 1997]. The free-carrier density may be calculated directly from the slope of these curves, which is n_{-2} .

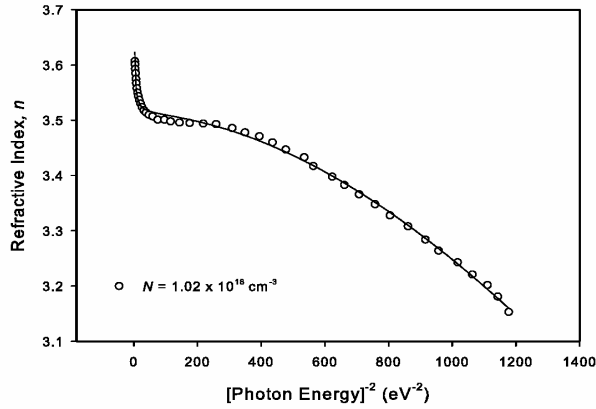


Fig. 12 Generalized Cauchy fit to the silicon index data of Schumann *et al.* for a carrier density of 1.02×10^{18} electrons cm^{-3} .

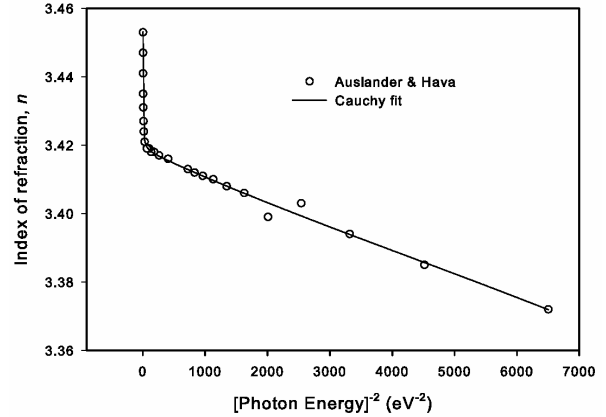


Fig. 13 Generalized Cauchy fit to the silicon index data of Auslander and Hava for a carrier density of 1.0×10^{16} electrons cm^{-3} . Note that the fit discloses two points that have been clearly transposed in the published data.

Most recently we have developed an analytic fitting procedure for the higher energy portion of core absorptions that is asymptotically correct at high energies. This has enabled us to correct a number of errors in the NTIS data base for the K-edge spectra and to place limits on the accuracy of the relative measurements of the near-edge absorption, which are given in the literature in arbitrary units. It has also allowed us to make what we believe to be a physically correct interpolation of L-shell absorption between 277 and 1486 eV, the region for which no measurements are available. With these data we addressed the long-standing problem of the average energy loss of charged particles in silicon which is discussed below.

For further details, see [Karstens 2006]

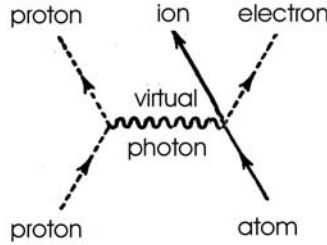
10. Stopping Power of Light Elements for Charged-Particle Radiation

An outstanding puzzle in radiation physics is the experimental and theoretical confusion surrounding the stopping power of silicon. The most recent experiments give values significantly higher than earlier experiments, and seem to be supported by Bloch's statistical atomic model. In contrast, earlier experiments are in accord with the observed trends found for other light elements. We have exploited our development of a composite set of optical constants for silicon to address this issue. In short, we have carried out a calculation originally suggested by Bethe for evaluating stopping power that was not feasible here-to-fore because of the lack of sufficient electromagnetic response data. We conclude that the more recent measurements are very likely in error and we have identified shortcomings in the statistical model that make it insensitive to details of atomic shell structure. The background is as follows.

Charged particles passing through matter lose their kinetic energy by electronic excitation of the atoms along their paths. This is the predominant process in absorption and shielding of radiation. Moreover, these electronic excitations are the initial step in radiation damage and

radiochemistry; the swarm of energetic primary and secondary electrons break chemical bond and the radiation-induced charged ions destabilize equilibrium crystal structures.

Energy loss in Coulomb collisions was first treated in a landmark paper by Bethe [Bethe 1930]. Qualitatively his insight was that as swift charged particles pass by an atom, the atom “sees” rapidly changing electric currents and fields. That is, electromagnetic transients or flashes of virtual photons for each particle. These “light pulses” contain a broad spectrum of photon energies and propagation directions that excite the atom and transfer part of the particles’ kinetic energy to the atomic electron(s). The cross section for this process is directly related to the materials’ optical properties because the probability of an excitation is given by the dielectric response. Schematically,



Bethe found that the *sole* material property that appears in the energy-loss cross section is the mean excitation energy, I , is defined by

$$\ln I = \int \ln E \frac{df_c}{dE} dE \Big/ \int \frac{df_c}{dE} dE . \quad (15)$$

In words, the atomic excitation energy E , weighted by the oscillator strength density, df_c/dE , for Coulomb excitations, which is proportional to the reciprocal of the dielectric function, $\epsilon(\omega)$,

$$\frac{df_c(\omega)}{dE} \propto -\omega \operatorname{Im} \left(\frac{1}{\epsilon(\omega)} \right) . \quad (16)$$

(The somewhat unexpected logarithmic form enters because the Fourier transform of the Coulomb interaction introduces a factors of k in the denominator and integration over scattering directions leads to a logarithm of $k = \omega/c$ that is then integrated over all energies.)

The practical difficulty with this formulation has been that the integrations cover the *entire range* of excitation energies and $\epsilon(\omega)$ remained poorly known except for small regions in the visible and that for only a few materials. Now measurements with synchrotron light sources have filled in the major gaps for a number of light elements. We have exploited this to carryout Bethe’s original program of evaluating I . For silicon we used the composite optical/x-ray data developed in this Partnership (see Section 9 above) and composites for carbon [Karstens 2004], and aluminum [Shiles 1980].

In the course of evaluating the Bethe formalism, we discovered the contribution of various atomic shells to I may be visualized by introducing the cumulative I value,

$$\ln I(E_{\max}) = \int_0^{E_{\max}} \ln E \frac{df_C}{dE} dE \Big/ \int_0^{E_{\max}} \frac{df_C}{dE} dE . \quad (17)$$

This new quantity is a measure of the I value as a function of the energy, E_{\max} , of the highest atomic level excited and, hence, of the cumulative contribution of electrons in each shell. Our results for aluminum and silicon are given in Figs. 14 and 15.

The graphs clearly show the importance of atomic shell structure, which is not present in statistical atomic models.

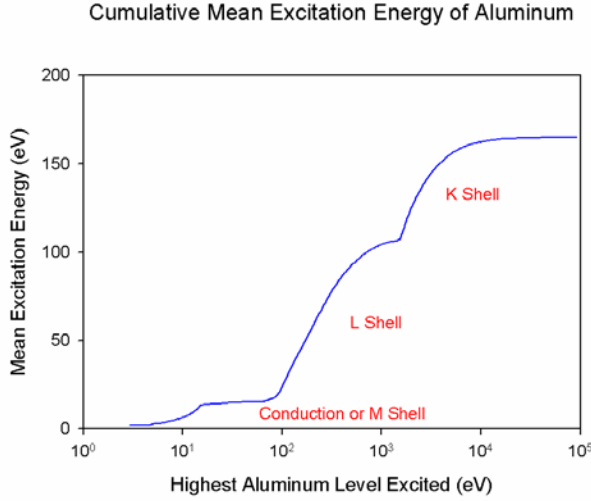


Fig. 14. Cumulative I value for aluminum metal calculated using the composite data of Shiles, *et al.* [Shiles 1980].

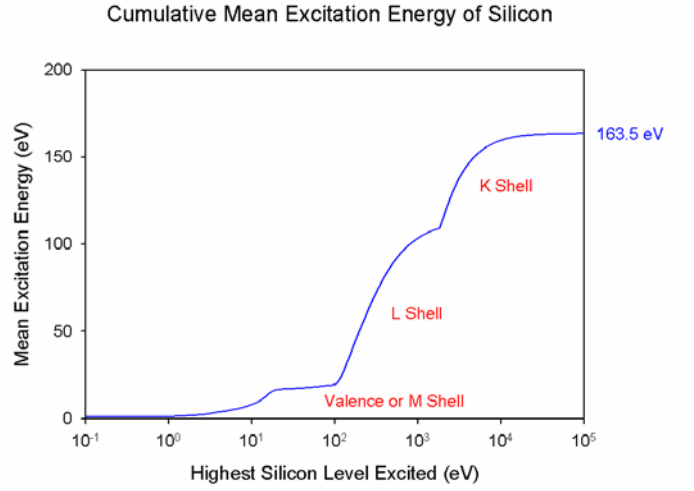


Fig. 15. Cumulative I value for crystalline silicon using the composite data of Inokuti Karstens, Shiles and Smith as found in the present project (see Section 9).

Qualitative these plots show us that the primary contributions to I are from the inner atomic shells, *not* the valence shell. Specifically,

- The K and L shells are the dominant contributors to I in light elements. Indeed, on a per-electron-basis, the two K -shell electrons make significantly larger contributions to I than do the eight L -shell electrons.
- Valence or conduction electrons, here the M shell, make little contribution to I . This explains the experimentally observed weak dependence of I on chemical bonding, and dispels the naive notion that plasmon excitation is of primary importance in energy loss. The ejected K - and L -shell electrons may create plasmons as they shed their kinetic energy, but this is a secondary process that does not contribute to the energy loss by the original radiation.

The results of evaluating I are given, along with values recommended by the ICRU [ICRU 1984], in Table I. The I values for carbon and aluminum derived from optical data are in

excellent agreement with current ICRU recommendations. The value for silicon, 164 ± 2 eV, differs substantially from the ICRU recommendation, 173 ± 3 eV, which is based on the more recent data, and from that of Tschalär and Bichsel [Tschalär 1968] who report 173.5 eV for proton energy loss. It is, however, consistent with the earlier experimental value of 164 eV reported by Andersen [Anderson 1977].

Element	Mean Excitation Energy, I (eV)	
	Optical & X-Ray Spectra, present study	Particle Energy Loss, ICRU Report 37
C	77 ± 4	78.0 ± 7
Al	165.7 ± 2	166 ± 2
Si	164 ± 2	173 ± 3

Remarkably, the I value for silicon found here from self-consistent composite optical data is equal to that for aluminum to within computation uncertainty. This is in sharp contrast to Bloch's statistical-atom result [Bloch 1930 a and b] that $I \propto Z$, which predicts the value should be 8% higher. At first the statistical-atom result would seem to favor the recent measurements, however, the present calculations shows our lower value reflects a real effect related to atomic shell structure. The reasons may be seen from Figs. 14 and 15, which show the importance of atomic shell structure, a feature ignored in statistical atomic models.

Stated differently, the near equality of the aluminum and silicon I values arises because

1. While the silicon K and L shells have greater excitation energies than those of aluminum, the additional weakly bound M electron in Si contributes so little that the *average* excitation energy does not change appreciably in going from aluminum to silicon; further,
2. The Pauli principle forbids transitions from core states to filled 3p states. The extra electron in Si reduces inner-shell absorption relative to Al. This is clearest for the K shell: Loss of a single $1s \rightarrow 3p$ transition reduces the K-shell strength from 1.61 to 1.55 e/a.

Aside from resolving a scientific conflict, our finding of a lower value of, $I_{\text{Si}} = 164 \pm 2$ eV brings the ICRU value, 173 ± 3 eV, into question and suggests use of this value for silicon-containing absorbers overestimates their effectiveness.

For further details, see [Smith 2006].

11. Literature Cited

- Alp, E. E. , M. Ramanathan, S. Salem-Sugui, Jr., F Oliver, V. Stojanoff, and D. P. Siddons 1991, *Rev. Sci. Instrum.* **63**, 1221.
- Tschalär, C. and H. Bichsel 1968, *Phys. Rev.* **175**, 476.
- Anderson, H. H., and J. F. Ziegler 1977, *Hydrogen Stopping Powers and Ranges in All Elements*, Pergamon Press, Oxford.
- Auslander, M. and S. Hava 1997, “Doped n-type silicon”, in *Handbook of Optical Constants of Solids vol. 3*, E. D. Palik, ed. Academic, New York p. 155.
- Bell, R. J., P. Dean and D. C. Hibbins-Butler 1974, *J. Phys. C: Solid St. Phys.*, **4**, 1214.
- Bennett, H. S. and E. A. Stern, 1965, *Phys. Rev.* **137**, A448.
- Bethe, H. 1930, *Ann. Phys. (Leipzig)* **5**, 325.
- Black, C. E. W. Karstens, D. Y. Smith 2005, *Bull. Am. Phys. Soc.* **50**, 1413.
- Bloch, F. 1933a *Ann. Phys. (Leipzig)* **16**, 287.
- Bloch, F. 1933b *Z. Physik.* **81**, 363.
- Boswarva, M., R. E. Howard and A. B. Lidiard 1962, *Proc. R. Soc. Lond. A* **269**, 125.
- Cauchy, A. L. 1836, *Mémoire sur la Dispersion de la Lumière*, Calve, Prague.
- Collins, S. P. 1999, *J. Phys.: Condens. Matter* **11**, 1159.
- Corning Inc. 2004, *ULE Glass Brochure*, Corning, Canton, NY.
- DiDomenico, M., Jr. 1972, *Appl. Opt.* **11**, 652.
- Frisch, M. J., G. W. Trucks, H. B. Schlegel, P. M. W. Gill, B. G. Johnson, M. A. Robb, J. R. Cheeseman, T. Keith, G. A. Petersson, J. A. Montgomery, K. Raghavachari, M. A. Al-Lahm, V. G. Zakrzewski, J. V. Ortiz, J. G. Foresman, J. Cioslowski, B. B. Stefanov, A. Nanayakkara, M. Challacombe, C. Y. Peng, P. Y. Ayala, W. Chen, M. W. Wong, J. L. Anderes, E. S. Repolgle, R. Gomperts, R. L. Martin, D. J. Fox, J. S. Binkley, D. J. Defrees, J. Baker, J. P. Stewart, M. Head-Gordon, C. Gonzales, and J. A. Pople 1995, *Gaussian 94, Revision C. 3*, Gaussian, Inc., Pittsburgh PA.
- Fukuda, A. 1964, *Science of Light* **13** 64.
- Gloge, D. 1971, *Appl. Opt.* **10**, 2252.

- Griscom D. L. 1985, *J. Non-Cryst. Solids* **73**, 51.
- Hirota, S., T. Izumitani, and R. Onaka 1985, *J. Non-Cryst. Solids* **72** 39.
- International Commission on Radiation Units and Measurements 1984, ICRU Report 37, *Stopping Powers for Electrons and Positrons*, ICRU, Bethesda.
- Izumitani, T. S. 1986, *Optical Glass* (Am. Inst. of Physics, New York).
- Karstens, W. and D. Y. Smith 2004, *Bull. Am. Phys. Soc.* **49**, 67 (2004).
- Karstens, W., D. Bobela, and D. Y. Smith 2006, *J. Opt. Soc. Am.* **23** [3], 723.
- Kirk, C. T. 1988, *Phys. Rev. B* **38**, 1255.
- Landau, L. D. and E. M. Lifshitz 1960, *Electrodynamics of Continuous Media*, Pergamon Press, Oxford.
- McWhan, D.B., J. B. Hastings, C. C. Kao, and D. P. Siddons 1992, *Rev. Sci. Instrum.* **63** 1404.
- McWhan, D. B. 1994, *J. Synchrotron Rad.* **1**, 83.
- Nakamoto, K. 1997, *Infrared and Raman Spectra of Inorganic and Coordination Compounds*, 5th ed. Wiley, New York.
- Osantowski, J. 1974, *J. Opt. Soc. Am.* **64**, 834.
- Pacchioni, G., L. Skuja, and D. L. Griscom (eds.) 2000, *Defects in SiO₂ and Related Dielectrics: Science and Technology* Kluwer, Dordrecht.
- Philipp, H. R. 1985, in *Handbook of Optical Constants of Solids, Vol. I*, E. D. Palik (ed.) Academic Press, New York, , pp. 719 and 749.
- Rife, J and J. Osantowski 1980, *J. Opt. Soc. Am.* **70**, 1513.
- Ribarsky, M.W. 1985 in: E. D. Palik (ed.), *Handbook of Optical Constants of Solids*, Academic, New York, p. 795.
- Schott 1995, *Catalog - Optical Glass*, Schott Glaswerke, Mainz.
- Schumann, P. A Jr., W. A. Keenan, A. H. Tong, H. H. Gegenwarth, and C. P.Schneider, 1970, *Optical constants of silicon in the wavelength range 2.5 to 40 μ m*, IBM Technical Report TR 22.1008.

- Schumann, P. A Jr., W. A. Keenan, A. H. Tong, H. H. Gegenwarth, and C. P. Schneider, 1971, *J. Electrochem. Soc.* **118**, 145.
- Shiles, E., T. Sasaki, M. Inokuti, and D. Y. Smith 1980, *Phys. Rev. B* **22**, 1612.
- Siddons, D. P., M. Hart, Y. Amemiya and J. B. Hastings 1990, *Phys. Rev. Lett.* **64**, 1967.
- Smith, D. Y. 1976a, *J. Opt. Soc. Am.* **76**, 454.
- Smith, D. Y., Mitio Inokuti and W. Karstens 2002, *Radiation Effects and Defects in Solids*, **157**, 823.
- D. Y. Smith 2003, *Bull. Am. Phys. Soc.* **48**, 194.
- Smith, D. Y., E. Shiles, and M. Inokuti 2004, *Nucl. Instr. and Meth. in Phys. Res. B* **218**, 170.
- Smith, D. Y., E. Shiles, and M. Inokuti 2005, *phys. stat. sol. (c)* **2**, 310.
- Smith, D. Y., M. Inokuti, W. Karstens, and E. Shiles 2006, *Nucl. Instr. and Meth. in Phys. Res. B* **250**, 1.
- Smith, D. Y., C. E. Black, C. C. Homes, and E. Shiles 2007, *phys. stat. sol. (c)* (in press).
- Tschalär, T. and H. Bichsel 1968, *Phys. Rev.* **175**, 476.
- Van Vleck, J. H. 1948, *Phys. Rev.* **74**, 1168.
- Wemple, S. H. 1979, *Appl. Opt.* **18**, 31.
- Yuster, P. H. and C. J. Delbecq 1952, *J. Chem Phys.* **21** 892.

Appendix A, Publications and Presentations During the Project Period

Articles in Reviewed Journals

- W. Karstens, and D. Y. Smith, *Defect Signatures in Dispersion Spectra*, Nucl. Instr. and Meth. in Phys. Res. B **191**, 44-47 (2002).
- D. Y. Smith, Mitio Inokuti and W. Karstens, *Cauchy's Dispersion Equation Reconsidered: Dispersion in Silicate Glasses*, Radiation Effects and Defects in Solids, **157**, 823-828 (2002).
- D. Y. Smith, E. Shiles, and M. Inokuti, *Refraction and Dispersion in Optical Glass*, Nucl. Instr. and Meth. in Phys. Res. B **218**, 170-175 (2004).
- D. Y. Smith, E. Shiles, and M. Inokuti, *Ultraviolet color centers and refraction in silicate glasses*, phys. stat. sol. (c) **2** [1], 310-313 (2005).
- W. Karstens, D. Bobela, and D. Y. Smith, *Impurity and Free-Carrier Effects on the Far-Infrared Dispersion Spectrum of Silicon*, J. Opt. Soc. Am. **23** [3], 723-729 (2006)
- D. Y. Smith, M. Inokuti, W. Karstens, and E. Shiles, *Mean Excitation Energy for the Stopping Power of Light Elements*, Nucl. Instr. and Meth. in Phys. Res. B **250**, 1-5 (2006).
- D. Y. Smith, C. E. Black, C. C. Homes, and E. Shiles, *Optical properties of $\text{TiO}_2\text{-SiO}_2$ glass over a wide spectral range*, phys. stat. sol. (c) (in press).

Abstracts of Conference Presentations

- D. Y. Smith and W. Karstens, *Dispersion Theory of Optical Glass*, Bull. Am. Phys. Soc. **47** [1, Part I], 293-294 [D28-2] (2002).
- W. Karstens, D. Bobela, and D. Y. Smith, *Effect of Impurities on the Far-Infrared Dispersion Spectra in Silicon*, Bull. Am. Phys. Soc. **47** [1, Part II], 992 [S17-4] (2002).
- D. Y. Smith, M. Inokuti, and W. Karstens, *Cauchy's Dispersion Equation Reconsidered: Dispersion in Silicon and Disordered Silicate Systems*, 9th Europhysical Conference on Defects in Insulating Materials (EURODIM), Wrocław 30 June - 5 July 2002.
- D. Y. Smith, *Dispersion Relations for X-Ray Faraday Rotation and Magnetic Circular Dichroism*, Bull. Am. Phys. Soc. **48**, 194 (2003).
- E. J. Shiles, M. Inokuti, W. Karstens, and D. Y. Smith, *Surface Effects and UV Optical Properties of Silicon*, Bull. Am. Phys. Soc. **48**, 890 (2003).

- D. Y. Smith, and M. Inokuti, *Refraction and Dispersion in Optical Glass*, 12th International Conference on Radiation Effects in Insulators, Gramado, Brazil, 31 August - 5 September 2003.
- W. Karstens and D. Y. Smith, *Optical Properties of Graphite*, Bull. Am. Phys. Soc. **49**, 67 (2004).
- E. Shiles and D. Y. Smith, *Refraction and UV Absorption in Optical Glass*, Bull. Am. Phys. Soc. **49**, 305 (2004).
- C. E. Black, M. Inokuti, W. Karstens, M. S. Malghani, E. Shiles, D. Y. Smith, *Synchrotrons Shed New Light on Optical Glass*, DOE/NSF- EPSCoR Conference 2004, Argonne National Laboratory, Argonne, IL, 14 June 2004.
- M. Inokuti, W. Karstens, E. Shiles, and D. Y. Smith, *Mean Excitation Energies for Stopping Power Evaluated from Oscillator-Strength Spectra*, Symposium on the Interaction between Particle Beams and Matter, Okayama University of Science, Okaama, Japan, 14-15 October 2004. (invited presentation)
- D. Y. Smith, E. Shiles, and M. Inokuti, *Ultraviolet color centers and refraction in Silicate Glasses*, International Conference on Defects in Insulating Materials, University of the Riga, Latvia, 11-16 July 2004.
- Mitio Inokuti, , W. Karstens, E. Shiles, and D. Y. Smith, *Mean Excitation Energy for the Stopping Power of Silicon from Oscillator-Strength Spectra*, Bull. Am. Phys. Soc. **50**, 1007 (2005).
- D. Y. Smith, W. Karstens, and M. S. Malghani, *Optical Constants Determined by Genetic Algorithms*, Bull. Am. Phys. Soc. **50**, 1075 (2005).
- C. E. Black, W. Karstens, D. Y. Smith, *Refractive-Index Dispersion Formulas, Old and New*, Bull. Am. Phys. Soc. **50**, 1413 (2005).
- E. Shiles, M. Inokuti, W. Karstens, and, D. Y. Smith, *Mean Excitation Energy for the Stopping Power of Silicon from Oscillator-Strength Spectra*, DOE/NSF- EPSCoR Conference 2005, National Energy Technology Laboratory, Morgantown, WV, 14-16 June 2005.
- D. Y. Smith, M. Inokuti, W. Karstens, and E. Shiles, *Mean Excitation Energy for the Stopping Power of Light Elements*, 13th International Conference on Radiation Effects in Insulators, SantaFe, NM, 28 August – 02 September 2005.
- W. Karstens and D. Y. Smith, *Analysis of Reflectivity Measurements*, Bull. Am. Soc. **51**, 705 (2006).
- C. E. Black, E. Shiles, *Contribution of IR Ionic Modes to the Refractive Index of Glasses*, Bull. Am. Soc. **51**, 1290 (2006).

D. Y. Smith, C. E. Black, C. C. Homes, and E. Shiles, *Optical Properties of Vitreous $\text{TiO}_2 - \text{SiO}_2$ over a Wide Spectral Range*, 10th Europhysical Conference on Defects in Insulating Materials (EURODIM 2006), University of Milano-Bicocca, Milano, Italy, July 10-14, 2006.

D. Y. Smith and W. Karstens, *Moments Formulation of Optical-Pulse Propagation in Insulators*, Bull. Am. Soc. **52** (in press).

Invited Presentations

D. Y. Smith, Optical Properties of Glass in a New Light,
Conference on Atomic Transport in Complex Materials
The Royal Institution of Great Britain, London, 27-28 June 2002.

D. Y. Smith, Transparent Materials in a New Light,
Physics Department Colloquium
Lehigh University, November 14, 2002.

D. Y. Smith, Ultraviolet Spectroscopy of Disordered Systems: Optical Glass,
Physics Department Colloquium
University of Vermont, April 14, 2004.

D. Y. Smith, Optical and Electronic Properties of Silicon and Silicate Glasses,
Segall Symposium
Department of Physics, Case-Western Reserve University, October 1, 2005.

Appendix B. Training and Support

Category	Number	Comments
Undergraduate major	1	Part-time student assistant, 4 years
Graduate Student	1	Part of one semester only
Postdoctoral Fellows	2*	Including the research-salary portion of a part-time research/part-time teaching post doc., and of an off-campus Research Associate at Argonne.

* In addition, a former postdoctoral fellow was recruited and mentored as a no-cost collaborator during his years as a probationary faculty member at a neighboring undergraduate college. His institution provided salary support, but the DOE EPSCoR program indirectly supported him with research supplies, and opened the way for summer collaboration with the PI and Dr. Inokuti at Argonne National Laboratory. Essentially, he served as a part-time senior postdoctoral fellow over the course of the whole project period.